

Preliminary Parallaxes for Cool Subdwarfs

Conard C. Dahn¹, Hugh C. Harris¹

¹*U. S. Naval Observatory, 10391 W. Naval Observatory Road, Flagstaff, Arizona, USA 86001-8521*

Abstract. Preliminary USNO CCD parallaxes are employed to locate 13 subdwarfs or subdwarf candidates with $M_v > 14.0$ in the M_v vs $V-I$, M_{K_s} vs $I-K_s$ and/or M_{K_s} vs $J-K_s$ absolute magnitude versus color diagrams. First parallax determinations are presented for the ultracool subdwarfs LEHPM2–59, LSR0822+17, LHS2100, and 2M1227–04.

1. Introduction

Cool subdwarfs are rare – and ultra cool subdwarfs (UCSDs; those with spectral types later than sdM7) are especially rare. The tabulation of UCSDs recently presented by Kirkpatrick et al. (2014) includes only 28 entries. However, further discoveries are anticipated from additional follow-up on ALLWISE candidates as well as from spectroscopic observations of UKIDSS/SDSS candidates being carried out with the Magellan Telescope and Gran Telescope Canarias (Zhang et al. 2013). To date only 10 UCSDs have luminosities established by trigonometric parallaxes, primarily from the USNO CCD and IR programs (Monet et al. 1992; Vrba et al. 2004), and from the IR work of Schilbach et al. (2009; hereafter, SRS09). In the present work we present preliminary USNO CCD parallaxes for 8 UCSDs. Included are first parallax determinations for 4 UCSDs. In addition, we present results for 5 subdwarf candidates – stars with $M_v > 14.0$ that have $V_{\text{tan}} > 150 \text{ km s}^{-1}$ yet apparently lack definitive spectroscopic clarification as to their dwarf versus subdwarf status. These results are used to place these stars in several absolute magnitude versus color diagrams (CMDs).

2. The Astrometric Results

Table 1 summarizes the basic data employed in the discussion which follows. The first column gives an abbreviated version of the star name; the second column gives our preliminary absolute parallax in mas; the V and $V-I$ photometry quoted in the third

and fourth columns are on the Cousins system and come from observations made in Flagstaff (except for LSR0822+17, SSS1444–20, and 2M1626+39 where values transformed from SDSS gri data are adopted). The J and K_s values given in the fifth and sixth columns, respectively, are from the 2MASS Point Source Catalog, supplemented by improved measures from SRS09. The absolute M_v and M_{K_s} are given in the seventh and eighth columns. The spectral types quoted in the ninth column come from the literature and the V_{\tan} values in the tenth column are calculated from our parallax results (second column) along with the proper motions measured in the parallax determinations.

Table 1. Astrometric and Photometric Data

Name	Pi	V	V–I	J	K_s	M_v	M_{K_s}	SpT	V_{\tan}
Ultra Cool Subdwarfs									
LEHPM2-59	10.5	19.91	3.07	15.52	14.76	15.02	9.87	esdM8	340
	± 0.5	± 0.03	± 0.02	± 0.05	± 0.11	± 0.11	± 0.15		± 16
LSR0822+17	8.5	20.41	3.22	15.72	15.62	15.06	10.27	usdM7.5	335
	± 0.6	± 0.07	± 0.07	± 0.06	± 0.22	± 0.17	± 0.27		± 24
LHS2100	18.6	19.36	3.46	14.27	13.63	15.71	9.98	sdMlate!	158
	± 1.2	± 0.02	± 0.02	± 0.03	± 0.05	± 0.14	± 0.15		± 10
SSS1013-13	18.2	20.11	3.78	14.62	14.40	16.41	10.70	sdM9.5	269
	± 0.5	± 0.04	± 0.04	± 0.03	± 0.08	± 0.07	± 0.10		± 7
2M1227–04	11.4	19.76	2.92	15.49	14.87	15.05	10.16	usdM8.5	224
	± 0.7	± 0.03	± 0.03	± 0.03	± 0.12	± 0.14	± 0.17		± 14
SSS1444-20	57.7	20.1:	4.6:	12.59	11.95	18.9:	10.76	d/sdM9	287
	± 0.7	$\pm 0.1:$	$\pm 0.2:$	± 0.01	± 0.01	$\pm 0.1:$	± 0.03		± 3
2M1626+39	30.6	21.83	4.95	14.43	14.46	19.26	11.89	sdL4	216
	± 0.6	± 0.05	± 0.10	± 0.01	± 0.01	± 0.07	± 0.04		± 4
LSR2036+50	23.1	18.82	3.53	13.62	12.96	15.64	9.78	sdM7.5	300
	± 0.4	± 0.02	± 0.03	± 0.01	± 0.02	± 0.04	± 0.04		± 5
Subdwarf Candidates									
LHS1157	16.4	19.82	3.70	14.09	13.32	15.90	9.40	dM6.0	234
	± 0.5	± 0.05	± 0.05	± 0.03	± 0.03	± 0.07	± 0.07		± 7
LHS1187	29.3	17.53	3.36	12.34	11.56	14.86	8.90	dM5.0	150
	± 0.5	± 0.03	± 0.02	± 0.02	± 0.02	± 0.04	± 0.04		± 3
LHS17	58.7	16.28	3.49	10.97	10.15	15.12	8.99	?	203
	± 0.6	± 0.05	± 0.07	± 0.02	± 0.02	± 0.03	± 0.04		± 2
LHS1462	26.0	17.72	3.30	12.70	11.90	14.79	8.97	?	154
	± 0.6	± 0.03	± 0.03	± 0.03	± 0.02	± 0.05	± 0.05		± 4
LHS243	38.7	16.32	3.13	11.51	10.74	14.26	8.68	?	193
	± 0.5	± 0.03	± 0.02	± 0.02	± 0.02	± 0.03	± 0.04		± 3

Parallax determinations for four of the UCSDs in Table 1 were presented earlier in SRS09. Their results (20.28 ± 1.96 mas for SSS1013–13; 61.67 ± 2.12 mas for SSS1444–20; 29.85 ± 1.08 mas for 2M1626+39; and 21.60 ± 1.26 mas for LSR2036+50) are in very satisfactory agreement with our values presented above. A lower precision parallax determination of

61.2 ± 5.1 mas for SSS1444–20 by Faherty et al. (2012) is in similarly good agreement. The Torino Observatory Parallax Program determination of 41.0 ± 1.2 mas for LHS243 (Smart et al. 2010) is likewise in satisfactory agreement with our result for that star.

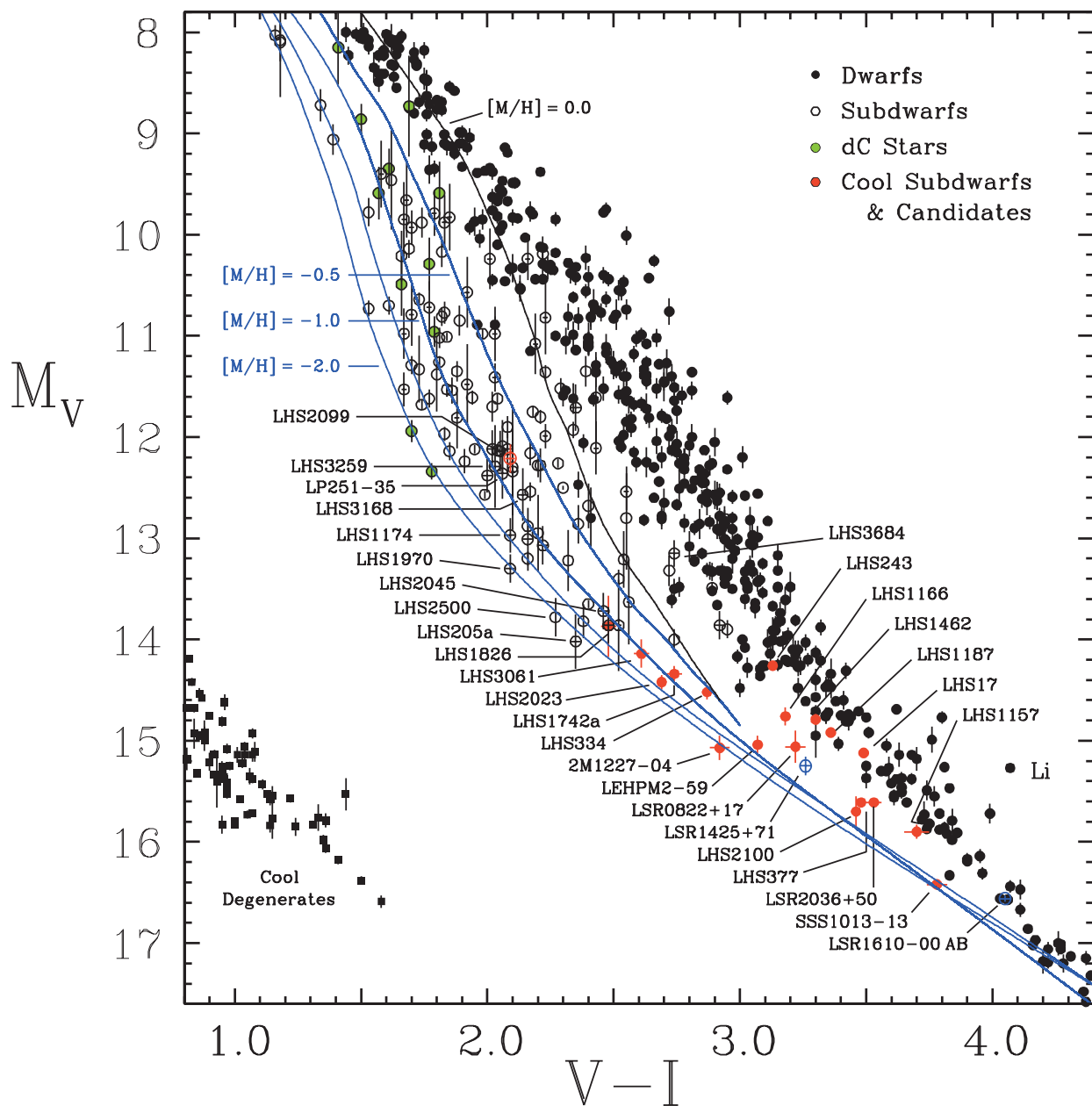


Figure 1: The M_V versus $V-I$ CMD. Table 1 stars are shown as filled red circles. See text for further details.

Figure 1 shows the locations of the Table 1 stars in the M_V versus $V-I$ CMD. This figure includes an ensemble of stars with $M_V > 8.0$ based on both published and unpublished

USNO CCD parallaxes and photometry. (All points are shown with formal $\pm 1\text{-}\sigma$ error bars in both coordinates.) Subdwarfs from Monet et al. (1992) – mostly with earlier spectral types, but including the benchmark UCSD LHS377 – are also labeled for reference and comparison. Model loci from Baraffe et al. (1997; 1998) are labeled for $[M/H]$ metallicity. Parallaxes and photometry for the UCSDs LSR1425+71 (sdM8.0) and LSR1610-00AB (d/sdM7:) are already in the literature (Dahn et al. 2008; SRS09). Both components of the LHS2099/2100 system were observed and the observations establish that the two stars indeed exhibit common proper motion and are at the same distance (within the combined errors of the determinations). Hence, in Table 1 we adopt the weighted mean of the parallaxes for the individual components. LHS2099 is an established esdM2.0 star (Gizis & Reid 1997) and its location in Fig.1 is indicated by the red open circle. The exact spectral type of LHS2100 has not yet been determined, but the star is clearly a late-type subdwarf (Bessell 1982; Phan-Bao & Bessell 2006). Not included in Fig.1 (due to scaling issues) are SSS1444-20 and 2M1626+39. The figure demonstrates that both the observational points and the models are converging rapidly at lower luminosities, such that for $M_v > 15$ there is only marginal dwarf versus subdwarf discrimination — and then only if accurate parallaxes are available. Based on the current astrometry, several stars which apparently lack definitive spectral types were noted as having tangential velocities in excess of 150 km s^{-1} . These five stars were examined further as “Subdwarf Candidates.” However, based on their locations in Fig.1 alone, there is no reason to suspect that they are metal-poor.

3. The M_{K_s} versus $I-K_s$ CMD

Figure 2 shows the location of the Table 1 stars in the M_{K_s} versus $I-K_s$ CMD. Other included stars are as described for Fig.1. Here the stars are labeled with their spectral types.

Table 2. Name versus Spectral Type Identifications

Name	SpecType	Name	SpecType	Name	SpecType
LSR1610-00AB	d/sdM7:	LHS192	esdM1.0	LHS1970	esdM3.0
SSS1444-20	d/sdM9	LHS3628	esdM1.5	LHS2045	esdM4.5
LHS334	sdM4.5	LHS3168	esdM1.5	LHS3390	esdM5.0
LHS1166	sdM6.5	LHS2099	esdM2.0	LHS1742a	esdM6.0
LHS377	sdM7.0	LHS3382	esdM2.5	LHS2023	esdM6.0
LSR2036+50	sdM7.5	LP251-35	esdM3.0	LHS1826	esdM6.0
LSR1425+71	sdM8.0	LHS1174	esdM3.0	LEHPM2-59	esdM8
LHS2100	Late sdM	LHS453	esdM3.0	LSR0822+17	usdM7.5
SSS1013-13	sdM9.5	LHS3178	esdM3.0	2M1227-04	usdM8.5
LHS3059	esdM0.0				

Table 2 provides a cross-reference between star names and their spectral types. The progression with spectral type among extreme subdwarfs labeled along the left-hand side of Fig.2 is generally consistent with decreasing luminosity for metallicity in the $-1.5 < [M/H] < -1.3$ range. However, interpreting the CMD at full-face value would suggest that the lower lumi-

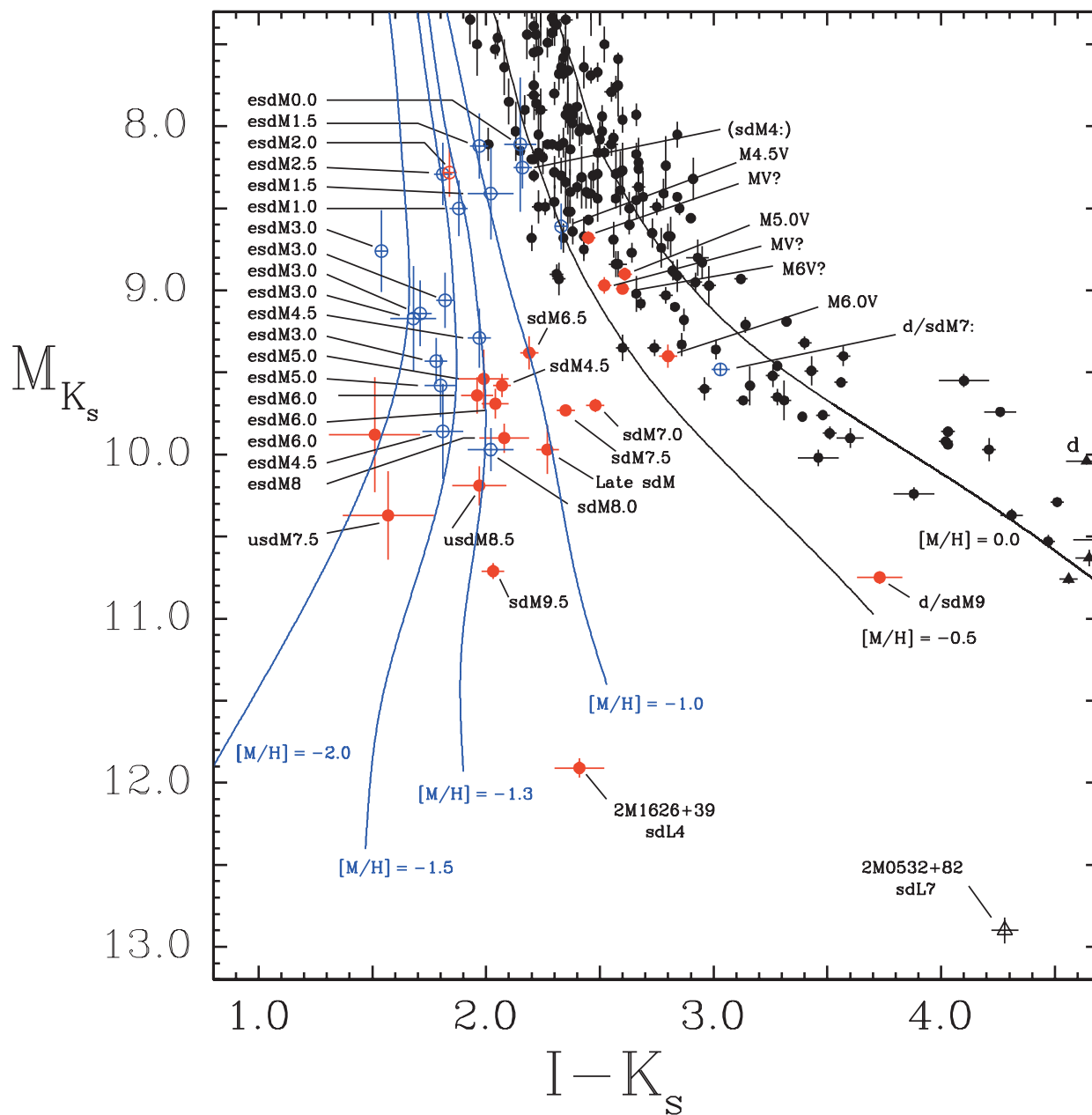


Figure .2: The M_{K_s} versus $I-K_s$ CMD. See text for details.

osity extreme subdwarfs have $-2.0 < [M/H] < -1.5$ and that the higher luminosity extreme subdwarfs have $-1.3 < [M/H] < -0.7$.

4. The M_{K_s} versus $J-K_s$ CMD

Figure 3 shows the location of the Table 1 stars in the M_{K_s} versus $J-K_s$ CMD. Again, the included stars are as described for Fig.1. Included in this CMD is the UCSD 2M0532+82, employing the weighted mean of the parallax determinations from the USNO IR program and from SRS09. Note that for several stars (e.g., LSR0822+17), the uncertainty in the adopted photometry (primarily for K_s) is a major contributor to the overall uncertainty in the final result.

5. Brief Discussion

There is an obvious lack of UCSDs with $M_{K_s} > 11$ in both Fig.2 and Fig.3. Given the paucity of L-type subdwarfs even identified to date – much less having trigonometrically derived distances – this is not surprising. To associate this with a fall-off in the luminosity function would be premature at this stage. Gaia will obtain parallaxes for significant samples of Ultra Cool M-type dwarfs and M-type subdwarfs. Distances out to 50–100 pc will be accessible for the M-dwarfs and out to 150–200 pc for the M-subdwarfs. For the L-dwarfs and L-subdwarfs the Gaia return is less assured. Early type L-dwarfs will only be measured out to distances of 30–40 pc, and mid/late L-dwarfs will be limited to those within 15–25 pc. Based on the luminosity of 2M1626+39 ($M_I \approx 14.3$; see Table 1), we anticipate Gaia measuring L-subdwarfs out to at least 70 pc.

Dieterich et al. (2014) argue that the break between stellar and sub-stellar masses (i.e., brown dwarfs) occurs in the region of spectral type L2.5V. Independently, Kirkpatrick et al. (2014) have suggested that a “gap” might exist for subdwarfs plotted in the $J-K_s$ versus $J-W2$ diagram, with early-L subdwarfs interpreted as hydrogen-burning stars and late-L subdwarfs interpreted as very high-mass brown dwarfs. Within an old, metal-poor population the substellar members would have cooled sufficiently to leave the mid-L subdwarfs relatively rare. Hopefully, Gaia will be able to address this issue as well.

And finally, we note that the five stars observed as subdwarf “candidates” based on their moderately high V_{tan} values appear in both Fig.2 and Fig.3 to be at most only modestly metal-poor, with $[M/H] \approx -0.4$.

Acknowledgements. We acknowledge observations made by other USNOFS astronomers.

References

- Baraffe, I., Chabrier, G., Allard, F., et al. 1997, A&A, 327, 1054
 Baraffe, I., Chabrier, G., Allard, F., et al. 1998, A&A, 337, 403
 Bessell, M.S. 1982, Proc.ASA, 4, 417
 Dahn, C.C., Harris, H.C., Levine, S.E., et al. 2008, ApJ, 686, 548
 Dieterich, S.B., Henry, T.J., Jao, W.-C., et al. 2014, AJ, 147, 94
 Faherty, J.K., Burgasser, A.J., Walter, F.M., et al. 2012, ApJ, 752, 56

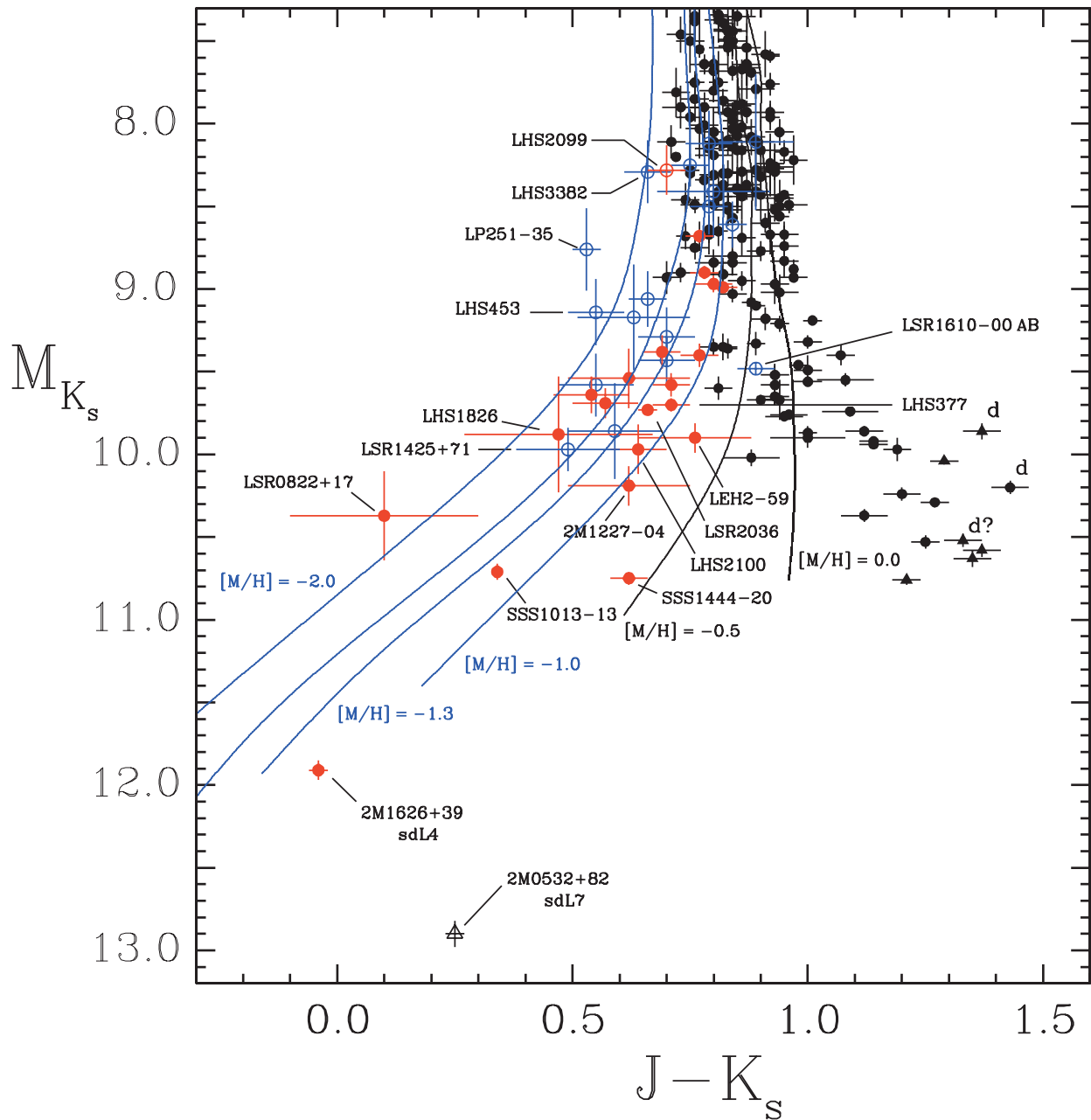


Figure .3: The M_{K_s} versus $J-K_s$ CMD. See text for details.

Gizis, J.E. & Reid, I.N. 1997, PASP, 109,

Kirkpatrick, D.J., Schneider, A., Fajardo-Acosta, S., et al. 2014, ApJ, 783: 122

Monet, D.G., Dahn, C.C., Vrba, F.J., et al. 1992, AJ, 103, 638

Phan-Ba0, N. & Bessell, M.S. 2006, A&A, 446, 515

Schilbach, E., Röser, S., & Scholz, R.-D. 2009, A&A, 493, L27; SRS09

Smart, R.L., Ioannidis, G., Jones, H.R.A., et al. 2010, A&A, 514, A84

Vrba, F.J., Henden, A.A., Luginbuhl, C.B., et al. 2004, AJ, 127, 2948

Zhang, Z.H., Pinfield, D.J. Burningham, B., et al. 2013, EPJ Web of Conferences 47, 06007



Part of the astrometry brain trust during CS18: (L to R) Trent Dupuy, Chris Tinney, Hugh Harris, Fred Vrba, and Conard Dahn.